Fragmentation dynamics of CS_2^{q+} $(q=3-10)$ molecular ions

F. A. Rajgara, M. Krishnamurthy, and D. Mathur
Tata Institute of Fundamental Research, Homi Bhabha Road, Mumbai 400 005, India

T. Nishide, T. Kitamura, H. Shiromaru, Y. Achiba, and N. Kobayashi
Graduate School of Science, Tokyo Metropolitan University, Tokyo 192-0397, Japan
(Received 27 April 2001; published 17 August 2001)

Dissociative ionization of highly charged CS_2^{q+} $(q=3-10)$ molecular ions produced in collisions of CS_2 with Ar^{8+} ions is studied at 120 keV energy. Triple coincidence techniques have been applied to measure the velocity components of all three ionic fragments produced in the fragmentation process. The velocity measurements have been used to deduce the total kinetic energy released (KER) in the fragmentation of the molecular ion for each particular product channel. KER values were found to be similar to those predicted by a pure Coulomb explosion model, revealing the apparent unimportance of binding electronic interactions in highly charged, multielectron molecular systems. The propensity of fragmentation into symmetric and asymmetric channels depends only on energetics, with the most exothermic channel being favored. The velocity vectors of the ion fragments yield information on ion structure prior to fragmentation; results indicate that the ionization is impulsive and fragmentation is simultaneous.

DOI: 10.1103/PhysRevA.64.032712 PACS number(s): 34.20.−b, 34.50.Gb

I. INTRODUCTION

Multiple-charged molecules are invariably unstable towards dissociation into charged atomic fragments, although barriers against dissociation can sometimes occur that lend a degree of metastability to low-lying electronic states [1]. This intrinsic instability is a consequence of the fact that the nuclear repulsion energy dominates over binding electronic energy and in certain cases, where there are avoided crossings of potential energy curves, results in metastability of the ions. The lifetimes of these metastable ions depend on the shapes of these potential-energy curves. This, in turn, leads to the consequence that both experimental and theoretical studies of such molecular species are difficult. From an experimental point of view, the production of the required ions and the study of the fragmentation that occurs on timescales as small as a few tens of femtosecond make mandatory the application of instrumentation techniques that have the capability of detecting, with adequate mass energy resolution and collection efficiency, coincidence spectra of two or more energetic fragment ions. From a theoretical viewpoint, the ability to adequately account for correlation energies, frequently involving inner-lying contracted orbitals in the molecular basis, poses a challenge to contemporary techniques of achieving convergence and developing efficient algorithms. Consequently, the need to gain deeper insights into the metastability of multiply charged molecules, the branching ratios between their different fragmentation pathways, and the distributions of kinetic energies released upon their fragmentation continues to play a major role in attempts to develop the practical ability of molecular quantum mechanics to generate reliable potential-energy surfaces.

From an applications angle, multiple-charged molecules are sources of energetic, charged, atomic fragments, and subsequent interactions involving these ions can lead to chemical modifications in the surrounding media. Consequently, such processes are of importance in the physics of plasma environments, both terrestrial as well as astrophysical, in atmospheric gases, on surfaces, and in radiological studies of biological systems. The dynamics of the fragmentation of multiply charged molecules is important, as a sensitive probe of electronic processes. It is now well established that in collisions of fast, highly charged ions with molecules, multielectron processes, like multiple ionization of the target molecule, play a very important role at large impact parameters, and that the energy-transfer process gives rise to situations where the recoiling target molecule may initially possess kinetic energies that are very small (less than one electron volt) whereas excitation energies of several kiloelectron volts are transferred to the target electrons. Such processes are important in areas such as radiation physics. For instance, electronic processes are mainly responsible for energy loss suffered by fast projectiles traversing biological matter, with water radiolysis being an important factor leading to cell death and cell mutation [2]. Even in crystalline matter, it is electronic energy that leads to the production of defects due to the displacement of atoms, even though it is not understood how the electronic energy is transformed into the kinetic energy of nuclei that finally results in the formation of tracks in the bulk material [3]. It has been suggested [4] that ion-induced fragmentation of multiple-charged molecules may be an example of how such energy transfer may proceed.

In general, the fragmentation of a multiple-charged molecule is referred to as a Coulomb explosion, but considerable experimental information exists to indicate that the kinetic energies of the fragment ions that are produced cannot, except in some cases, be explained in terms of a simple Coulombic process [5]. Non-Coulombic potential-energy surfaces of electronic states of multiple-charged molecules have been explored and are found to be essential in order to rationalize the deviations that might be observed from a Coulombic model [6,7]. On the other hand, experimental evidence also exists for purely Coulombic fragmentation. Early mea-

surements of kinetic energies released upon fragmentation of multiple-charged diatomics [8] were found to be in reasonable accord with predictions of a simple Coulomb explosion model wherein, for a diatomic molecule, the final kinetic energy (in electron volts) of the two fragment ions is equal to the initial Coulomb repulsion energy, $14.4q_1q_2/r$, where q_1q_2 are the asymptotic charges of the two fragments and r is the equilibrium internuclear distance (in angstrom). However, later experiments showed that single-valued fragment ion kinetic energies were not obtained and that there might be significant deviations from Coulombic energy values [9]. These deviations were interpreted in terms of either weaker screening of the nuclear charge by excited electrons or by non-Coulombic potential-energy curves of multiple-charged molecules [6]. Recently, fragment ion momentum spectrometry has been applied to the study of CO^{2+} fragmentation into C^+ and O^+ pairs. The experimental results from this study, which were interpreted with the aid of sophisticated time-dependent wave-packet dynamics computations utilizing *ab initio* potential-energy curves, dramatically reveal the limitations of the simple Coulomb explosion model [4].

Efforts to gain insight into the complex dynamical properties of multiple-charged molecules have received considerable impetus from recent advances in the technology associated with the simultaneous detection, identification, and analysis of all charged fragments produced upon fragmentation of such species. The ability to determine the velocity vectors of all the ionic fragments simultaneously in each dissociation event gives a complete insight into the dynamics of the process and reveals the mechanism involved in the interaction. For instance, one can get structural information on the molecular ion just prior to fragmentation. This can be applied to probe the transition state involved in the fragmentation of complex molecular systems. Access to structural information on the transition state is a key to unraveling many of the details of the overall dynamics.

Applications of triple coincidence techniques using a position-sensitive detector have been made to study the fragmentation dynamics of N_2, H_2O [10], CO_2, and NO_2 [11]. In these experiments, the bond angle of H_2O was well reproduced from the fragment ion velocity vectors that were measured. The other two triatomics that have been studied so far are more interesting, in that the dynamics is more complicated, because of the possibility of forming the three fragments in a variety of charge states. The triple coincidence signals for these molecules were identified for dissociation of CO_2^{q+} $(q=3-6)$ and NO_2^{q+} $(q=3-5)$. Velocity vectors of each fragment ion were measured for individual collision events, and the angles between the velocity vectors were deduced. For molecules in the highest charge states, these angles were found to be consistent with the angle that is spectroscopically known for the respective neutral molecule. In the case of lower charge states, however, some deviation was found from the neutral molecule bond angles. It was, consequently, postulated that the pure Coulombic dissociation process is applicable for the very highest charge states, in agreement with findings of the comparison made between experimental and quantum-chemical data made earlier by Mathur and co-workers [6].

We have now extended the scope of the triple coincidence measurements by studying the dissociation dynamics of highly charged carbon disulfide molecules in which two of the atoms are substantially heavier (and contain more electrons) than in species that have hitherto been studied. In this paper, we focus attention mainly on the energetics of the fragmentation process. We address the question whether a purely Coulombic dissociation is valid even for very high-molecular charge states CS_2^{q+}, with q as high as 10. The CS_2 molecule has a low single-ionization energy (10.08 eV) compared to the few molecules that have been the subject of earlier studies. We measure the fragmentation of the highly charged molecular ion, CS_2^{q+} into those channels that give rise to three charged atomic fragments, S^{a+}, C^{b+}, and S^{c+}. The velocity vectors of each of these fragment ions is measured and the kinetic energy released (KER) is experimentally determined. *Ab initio* quantum computations are employed to calculate KER values for specific fragmentation channels. Comparison between measured and calculated KER values reveals the importance of electronic excitation of the CS_2^{q+} molecular ion. Our results also show that the propensity of fragmentation into symmetric and asymmetric channels depends only on energetics, with the most exothermic channel being the one that is favored. The Coulomb explosion model holds very well for all the charge states of CS_2 that are studied here.

The measured velocity vectors of the fragment ion are used to obtain information on the structure of the molecule prior to fragmentation. The measured bond angle and χ angle of the molecular ion reveal that the fragmentation occurs in a concerted mechanism for all the product channels.

II. THE CS_2 MOLECULE

The equilibrium C-S bond lengths in the ground electronic state of CS_2 are 1.55 Å. From infrared spectroscopy it is established that the bending-mode vibrational frequency in the $X\,^1\Sigma_g$ state is 397 cm^{-1}. It would be expected that a certain fraction of CS_2 molecules in the ion-molecule interaction zone will, at the moment of impact with the highly charged ions (HCI) beam, have the central C atom displaced from the equilibrium linear geometry by the bending-mode vibrational amplitude. Using a simple harmonic oscillator model, the most probable instantaneous value of the angle between the two C-S bonds is known to be 175.2° for the $\nu=0$ vibrational level. At room temperature, the ratio of the vibrationally excited state ($\nu=1$, bending mode) to the ground state is about 0.3, not negligible amount. The most probable value of the bond angle for the $\nu=1$ level is 171.7°.

The ground electronic state of CS_2 has the electronic configuration

$$(\text{core})^{22}(5\sigma_g)^2(4\sigma_u)^2(6\sigma_g)^2(5\sigma_u)^2(2\pi_u)^4(2\pi_g)^4,$$

which yields an overall symmetry of $^1\Sigma_g^+$. Unlike most of the orbitals, which are C-S bonding in character, the outermost $2\pi_g$ orbital is mostly built up with $3p$ atomic orbitals

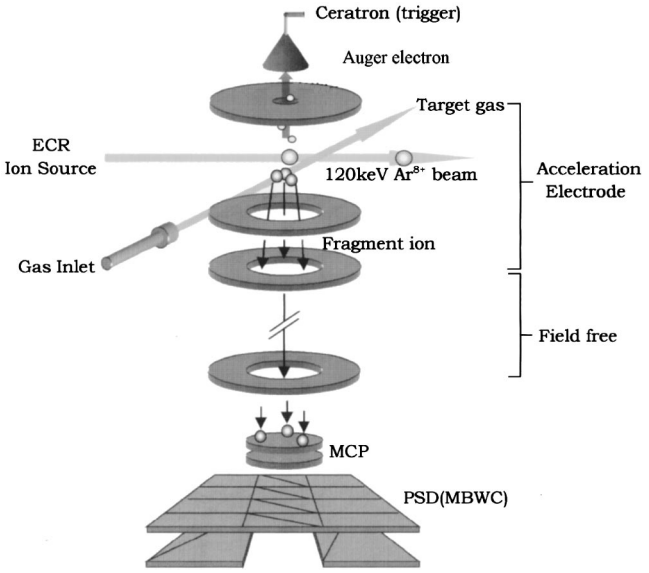

FIG. 1. Schematic representation of the experimental apparatus. MCP, microchannel plate detector; PSD (MBWC), position-sensitive detector with modified backgammon weighted capacitor anode; ECR, electron cyclotron resonance ion source.

of the sulfur atoms; as the equilibrium separation is large, there is relatively little π overlap between the two peripheral atoms and, consequently, little bonding. Removal of one or more of the four electrons in this orbital is, therefore, likely to result in a fragmentation process that is dominant Coulomb interaction.

III. EXPERIMENTAL SETUP

Our experiments were conducted using a crossed-beam, Coulomb explosion imaging apparatus whose essential features have been briefly described earlier [12] except that larger microchannel plate (MCP) detectors were also used in the present experiments. A beam of highly charged ions (HCI) (Ar^{8+} at 120 keV) is produced using a 14.25 GHz, electron cyclotron resonance ion source(TMU-ECRIS). The extracted HCI beam is then focused by a three-element electrostatic einzel lens, analyzed by a sector magnet according to their mass-to-charge ratio, and transported to a collision chamber using a beam transport system comprising electrostatic steerers and deflectors. The mass-analyzed HCI beam is collimated using an aperture of 2 mm diameter and made to cross, at right angles, a molecular gas beam of CS_2 effusing through a multicapillary plate. A turbo-molecular pump was used to base pressures of 6×10^{-9} Torr; typical working pressures were $\sim8\times10^{-7}$ Torr with CS_2 gas load. A schematic diagram of the apparatus is shown in Fig. 1.

In our experiments, multiple ionization of CS_2 occured as a result of the interaction with the HCI beam. Fragment ions formed upon dissociation of highly-charged states of CS_2 were electrostatically deflected into a linear time-of-flight mass spectrometer (TOFMS) using an extraction field of 360 $V\,cm^{-1}$ applied in a direction that was orthogonal to both the incident HCI beam and the target molecular beam. Auger electrons emitted by the projectile were detected by a Ceratron multiplier, giving rise to fast timing pulses that served as a start trigger for our TOF measurements. The mass-to-charge analyzed fragment ions were detected by 40 mm diameter microchannel plate detector coupled to a ''modified backgammon with weighted coupling capacitors'' (MBWC) anode. The anode divided the charge incident on it in terms of x and y coordinates in a manner that has been described elsewhere [13]. Some of the measurements on the highest charge states were also made with a 120 mm diameter microchannel plate detector in order to confirm that the large KER values reported here for CS_2^{q+} $(q>7)$ were measured with sufficient detection/collection efficiency.

IV. RESULTS AND DISCUSSION

A. Time and position measurements

The results that we report here concern the dissociation process that occurs when the CS_2 molecule interacts with Ar^{8+} ions. We focus attention on the Coulomb explosion of the highly charged CS_2^{q+} ion that is formed in this interaction and we monitor those dissociation channels that result in three fragment ions. An example of one such interaction is shown below.

$$Ar^{8+}+CS_2\rightarrow CS_2^{3+}\rightarrow S^+ + C^+ + S^+. \qquad (1)$$

We recorded the spatial positions (x_i,y_i) and flight time (t_i) of all three fragment ions relative to the start electron. If the number of ions detected by a single trigger is less than three, then those data are not recorded. The position-output signals, along with the timing information, were fed to a four-channel digital storage oscilloscope after preamplification using fast preamplifiers. The data were then transferred to a computer via a fast bus; the x,y position of each incident ion was determined from the relative heights of the pulses recorded on each channel.

B. 3D velocity mapping

The measured flight times and positions of the fragment ions enabled us to generate three-dimensional (3D) velocity vectors using the following methodology. The triple coincidence signals of the fragment ions (comprising electron-ion-ion-ion signals) were assigned to the corresponding dissociation channels of CS_2^{q+} $(n=3-10)$. Hereafter, the notation (a,b,c) indicates the dissociation channel $CS_2^{q+}\rightarrow S^{a+}+C^{b+}+S^{c+}$, where $a+b+c=q$. From the TOF's of each of the fragment ions, z components of the velocity vectors were determined; the position information yielded x and y components of the velocity vector for each fragment ion formed by a single dissociation event.

The x,y image obtained in the present paper was found to be slightly deformed on the periphery of our MCP. Although this did not induce any obvious (visible) distortion of the derived velocity vectors, we took the precaution of excluding all ion signals that were detected in the peripheral 1.5 mm area of our MCP in order to avoid possible systematic error in the results discussed later in this paper. Moreover, as stated above, some of the measurements were also repeated

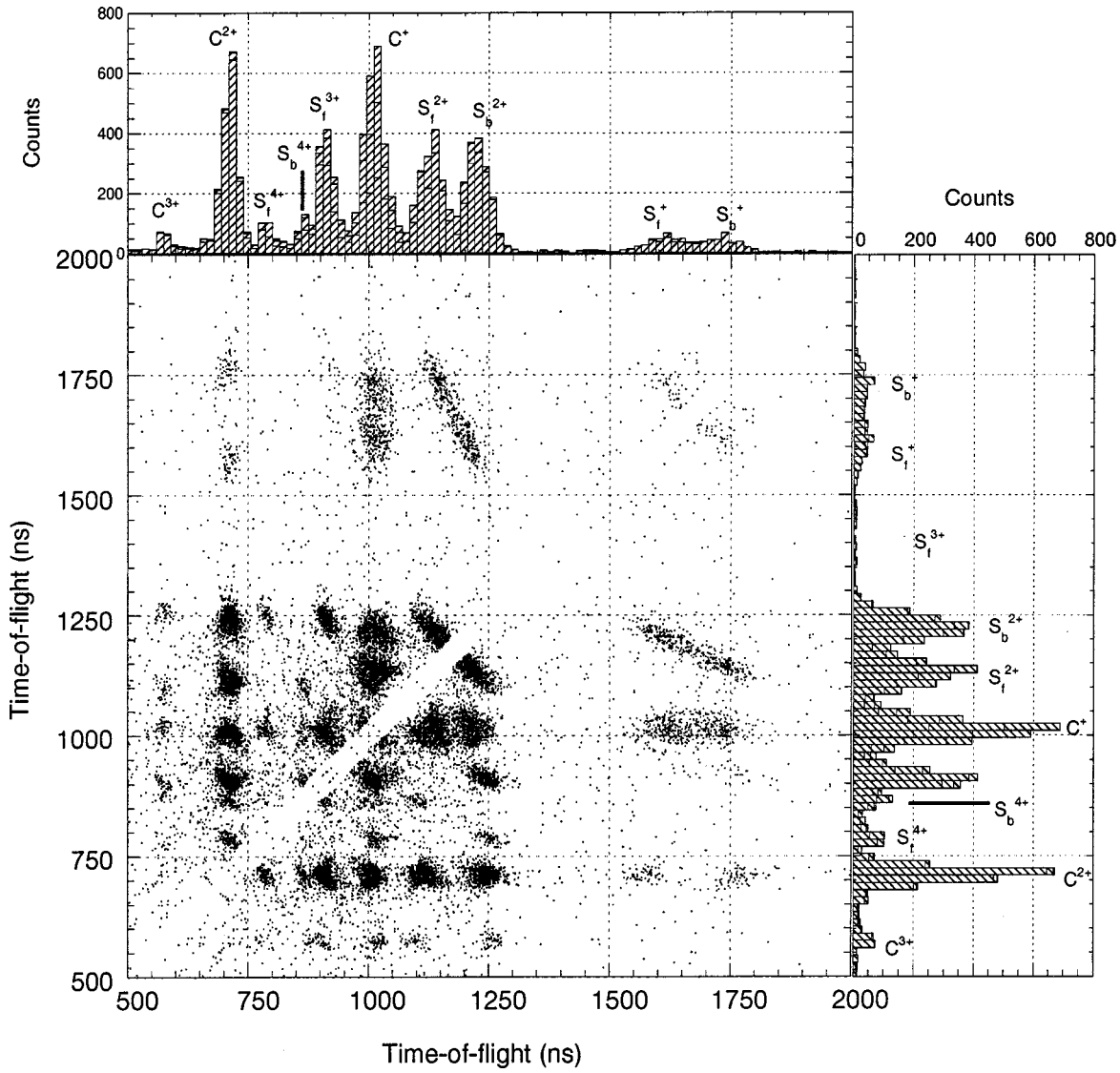

FIG. 2. Triple coincidence map of fragment ions produced in collisions of Ar^{8+} with CS_2. Time-of-flight spectra with identified fragment ions are also shown (see text).

using a larger, 120 mm diameter detector. In addition to this, the yields of some dissociation channels were underestimated due to a limitation of detection efficiency arising from the following factor. Although the time resolution of the measurement system was 2 ns, if two ions were to hit the detector within very short time difference, the positional accuracy would be lowered. To avoid possible systematic error, the events in which two ions hit within 20 ns were, therefore, excluded from further analysis. This discrimination is particularly of importance when, for instance, the charge state of the two S-ions is the same, or in cases where the dissociation events involve S^{3+} $(m/q=10.7)$ and C^{+} $(m/q=12)$ coincidences [that is, the (3,1,3) channel]. We took special care in the determinations of yields of these dissociation channels.

C. Coincidence maps

Figure 2 shows a typical coincidence map measured in our experiments using Ar^{8+} projectile ions at a collision energy of 120 keV. The possibility of false coincidences is minimized by maintaning very low count rates. Typically, the count rate was maintained at less than 1 count s^{-1}. Each point in the map is due to a coincidence signal of three ions. The density of points that give rise to dark patches, or islands, represent different fragmentation channels as highly charged CS_2^{q+} $(q=3-10)$ precursors formed in the ion-molecule interaction breakup. The figure also shows conventional TOF spectra of the fragment ions.

In order to illustrate the type of information that the coincidence maps yield, we consider the way to deduce the information due to the (2,2,2) channel. Consider a vertical cut through the point in the map that corresponds to the C^{2+} fragment. The spectrum that results is depicted in Fig. 3(a) and shows sulfur ions (in different charge states) that are formed in coincidence with the C^{2+} fragment; these represent the $(x,2,y)$ dissociation channel, where x, $y=1-4$. For each charge state, there are two peaks that are denoted by

subscripts *f* and *b*, representing, respectively, those fragment ions that were ejected in an initial direction toward, and away from, the detector (corresponding to ''forward'' and ''backward''-scattered ions in collision physics parlance). It should be noted that the absence of signals between the forward and backward was due to the fact that we excluded the event in which two S^{2+} ions arrived at the detector within 20 ns. Further reduction of data was carried out by choosing subsets of specific channels. For instance, Fig. 3(b) shows the spectrum of those ions that are also produced in coincidence with the S_f^{2+} fragment, yielding the $(2,2,y)$ channel, where $y=1-4$. The specific $(2,2,2)$ channel was then obtained from the points under the S_b^{2+} ion in Fig. 3(b). The time difference between the forward and backward scattered yielded information on the *z* component of the inital velocity of the fragment ion v_z. The kinetic energy of all the ions in the fragmentation event were obtained by summing $mv^2/2$ for x,y,z components, and the total kinetic energy released in the breakup of the molecular ion was obtained for each charge state of the molecular ion. We note that the data do not show ''forward'' and ''backward'' splitting in the case of C^{q+} ions, indicating that very little energy is imparted to the central carbon nucleus in the fragmentation process.

D. Values of kinetic energy released (KER)

We present the measured KER data for those fragmentation channels that lead to formation of three atomic ions from precursors CS_2^{3+} to CS_2^{10+} in Table I, and in Fig. 4. We have made a comparison with the values of KER that would be expected if a simple Coulomb explosion picture were valid. For CS_2^{q+} $(q=3-6)$, the quantum calculated values of KER are significantly lower than the measured ones. For higher charge states, this difference is no longer very significant. Comparison between the measured and Coulombic KER values reveals a major finding of the present paper: the measured KER values are reasonably close to those predicted by the Coulomb explosion model, for all CS_2 charge states, irrespective of the product channel. This finding reveals, somewhat surprisingly, the apparent unimportance of binding electronic interactions in highly charged, multielectron molecular systems. We note that in the case of CS_2^{9+}, the measured values of KER are substantially lower than the Coulombic and calculated ones. This probably reflects the inability of even our large size-detector system to efficiently collect all the energetic fragment ions that are produced. This is also true for CS_2^{10+} although the number of events assigned to these channels are quite few. As indicated in Table I, dissociation of CS_2^{10+} ions yields fragment ions whose kinetic energies are as large as 200–250 eV.

In order to gain further insight into the significance of our experimentally measured values of KER, we have also carried out high-level, *ab initio*, quantum-chemical calculations of the vertical excitation energies and dissociation limits of low-lying electronic states of CS_2^{3+} to CS_2^{10+} ions. All-electron, self-consistent-field (SCF) molecular orbital computations were carried out using second-order Möller-Plesset perturbation theory (MP2 level) to account for configuration interaction effects. The basis set used, 6-311G**, consisted

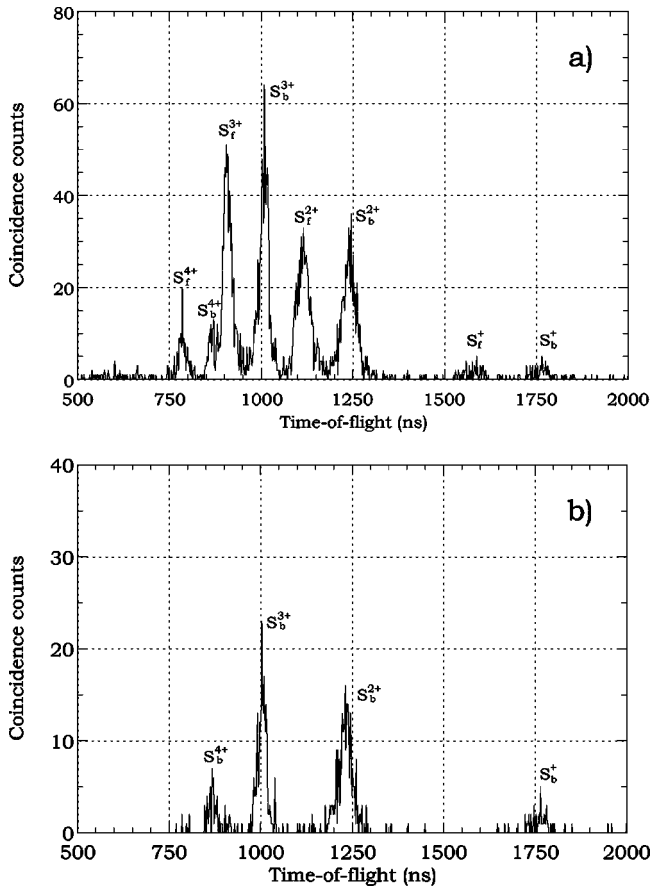

FIG. 3. (a) TOF spectrum of fragment ions produced in coincidence with C^{2+} ions; (b) TOF spectrum of ions produced in coincidence with C^{2+} and S_f^{2+} ions.

of $4s$, $3p$, and $1d$ functions for carbon, and $6s$, $5p$, and $1d$ functions for sulfur. These sets were obtained by appropriate splitting of the basis and by adding polarization functions to the original Gaussian basis sets of Huzinaga [14]. We carried out SCF calculations with a direct-minimization algrorithim in order avoid convergence problems [15].

We first determined the geometry of the neutral molecule in the ground electronic state, and performed single-point computations at the optimized geometry in order to deduce values for the vertical excitation energies to the lowest two electronic states, of different multiplicity, of each of molecular charge states CS_2^{q+} $(q=3-10)$. To determine the asymptotic limit for fragmentation from a given charge state, we also computed the energies of C^{q+} and S^{q+} ions. These values are tabulated in Table II. Knowing the dissociation limit and the vertical excitation energy of the molecular ion, we deduced the values of KER that would be obtained if dissociation were to occur via ''real'' non-Coulombic potential-energy surfaces. These calculated values of KER are also shown in Table I and depicted in Fig. 4 to serve as a useful guide to gauging the differences between the measured and Coulombic KER values.

The vertical excitation energies for CS_2^{q+} yield the ionization energy (IE) for these charge states. The experimental IE values are known for *q* values up to three, and we compare those with the computed values in Table II in order to estab-

TABLE I. Calculated, measured, and Coulombic values of kinetic-energy released (KER), in eV, obtained upon fragmentation of CS_2^{q+} molecular ions in given charge state q and multiplicity. The energy of each electronic state is the result of a calculation carried out at the equilibrium internuclear distance in the neutral molecule.

					KER		
Charge q	Multiplicity	Energy (H)	Dissociation channel	Dissociation limit (H)	Calc. (eV)	Meas. (eV)	Coulombic (eV)
3	2	−831.491	(1,1,1)	−831.862	10.1	19.5	23.1
	4	−831.382	(1,1,1)	−831.862	13.1	19.5	23.1
4	1	−830.288	(2,1,1)	−831.017	19.8	37.7	37.0
	3	−830.159	(2,1,1)	−831.017	23.4	37.7	37.0
5	2	−828.649	(2,1,2)	−830.172	41.5	56.9	55.5
	4	−828.589	(2,1,2)	−830.172	43.1	56.9	55.5
	2	−828.649	(2,2,1)	−830.132	40.4	59.8	64.7
	4	−828.589	(2,2,1)	−830.132	42.0	59.8	64.7
6	1	−826.755	(3,1,2)	−828.905	58.5	74.2	74.0
	3	−826.754	(3,1,2)	−828.905	58.5	74.2	74.0
	1	−826.755	(3,2,1)	−828.865	57.4	93.6	87.8
	3	−826.754	(3,2,1)	−828.865	57.5	93.6	87.8
	1	−826.755	(2,2,2)	−829.287	68.9	90.9	92.5
	3	−826.754	(2,2,2)	−829.287	68.9	90.9	92.5
7	2	−824.566	(4,1,2)	−827.181	71.1	107.8	92.5
	4	−824.551	(4,1,2)	−827.181	71.6	107.8	92.5
	2	−824.566	(3,1,3)	−827.638	83.6	91.6	97.1
	4	−824.551	(3,1,3)	−827.638	84.0	91.6	97.1
	2	−824.566	(3,2,2)	−828.020	94.0	118.3	120.2
	4	−824.551	(3,2,2)	−828.020	94.4	118.3	120.2
	2	−824.566	(2,3,2)	−827.531	80.7	125.2	129.4
	4	−824.551	(2,3,2)	−827.531	81.1	125.2	129.4
8	1	−821.907	(4,1,3)	−826.318	109.0	114.1	120.3
	3	−821.939	(4,1,3)	−826.318	108.2	114.1	120.3
	1	−821.907	(4,2,2)	−826.296	119.4	134.2	147.9
	3	−821.939	(4,2,2)	−826.296	118.6	134.2	147.9
	1	−821.907	(3,2,3)	−826.754	131.9	153.5	152.6
	3	−821.939	(3,2,3)	−826.754	131.0	153.5	152.6
	1	−821.907	(3,3,2)	−826.265	118.6	149.8	166.4
	3	−821.939	(3,3,2)	−826.265	117.7	149.8	166.4
9	2	−819.035	(4,1,4)	−824.190	142.7	141.1	148.0
	4	−818.944	(4,1,4)	−824.190	140.3	141.1	148.0
	2	−819.035	(4,2,3)	−825.029	163.1	147.8	177.1
	4	−818.944	(4,2,3)	−825.029	165.6	147.8	177.1
	2	−819.035	(3,3,3)	−824.998	162.3	180.4	208.0
	4	−818.944	(3,3,3)	−824.998	164.7	180.4	208.0
10	1	−815.753	(4,2,4)	−823.305	205.5	180.6	221.9
	3	−815.699	(4,2,4)	−823.305	207.0	180.6	221.9
	1	−815.753	(4,3,3)	−823.273	204.6	166.2	249.6
	3	−815.699	(4,3,3)	−823.273	206.1	166.2	249.6

lish a measure of the accuracy of our computed results. The comparison between computed and experimental atomic and molecular-ion data in Table II demonstrate that the methodology adopted by us is adequate for the purpose of comparing experimental and calculated KER values. The higher charge states would be expected to lead to even more contracted molecular orbitals, and since the inner orbitals are well represented in the basis set chosen by us, the results are expected to compare well even for the higher charge states.

Note that in Table I, results for CS_2^{q+}, $q \geqslant 3$, are presented for two multiplicities. For instance, in the case of CS_2^{6+} precursors, the vertical excitation energies were calculated for the lowest-lying singlet as well as triplet electronic states, and KER values were deduced for the symmetric (2,2,2)

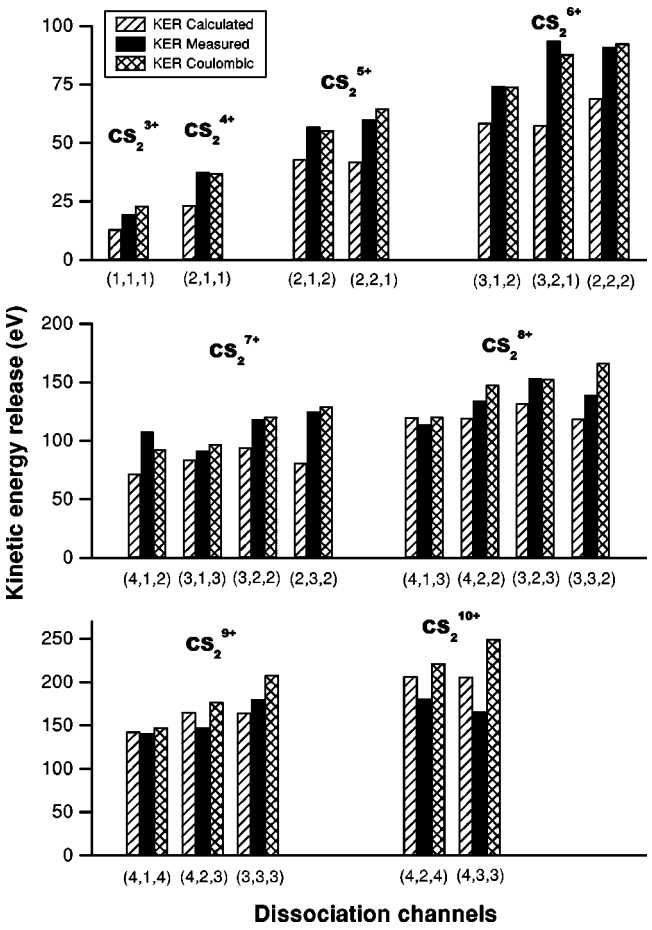

FIG. 4. Histograms of calculated, measured, and Coulombic KER values for various fragmentation channels, for different molecular ion charge states. KER values were computed for different electronic states of CS_2^{q+}. The calculated values shown here represent the largest of the values that were calculated (see Table I and text).

breakup channel as well as for the asymmetric channels (3,2,1) and (3,1,2). We have computed KER values for fragmentation by electronic state with different multiplicities of the CS_2^{q+}. Figure 4 compares the measured and Coulombic KER values with the calculated KER's values for higher-spin multiplicity. Similar comparison can also be done using the calculated KER values for lower spin multiplicity.

Careful analysis of the data depicted in Table I, and in Fig. 4, enable us to offer the following comments. The experimentally deduced values of KER are more or less the same as the Coulombic values, and, in most cases, more than the calculated ones. In this connection, it is important to note that the calculated KER values pertain to the lowest possible electronic state of a given symmetry and multiplicity. The calculated KER value, therefore, represents a lower limit. Population of higher electronic states of CS_2^{q+} is certainly possible, and KER's resulting from fragmentation of such states would be expected to narrow the apparent gap between measured and calculated values. However, the SCF procedure adopted in this calculation necessarily gives us the lowest electronic state of a given multiplicity and orbital angular momentum. Higher electronic states of the same symmetry are possible with more sophisticated multireference configuration interaction calculations, but those were not attempted here. Our results offer strong evidence for the formation of precursor ions in electronically excited states and this constitutes the second major finding of our study.

TABLE II. Computed energies of S ions, C ions, and CS_2 ions in various charge states. IE represents calculated and experimental values of ionization energies.

			Ionization energies	
Fragment ion	Charge q	Energy (H)	Calc. (eV)	Expt. (eV)
S	0	−397.5998		
	1	−397.2499	9.52	10.36
	2	−396.4048	23.0	23.33
	3	−395.1380	34.47	34.83
	4	−393.4136	46.92	47.30
C	0	−37.7667		
	1	−37.3625	11.00	11.26
	2	−36.4775	24.08	24.38
	3	−34.7219	47.77	47.89
CS_2	0	−833.372		
	1	−833.020	9.60	10.08
	2	−832.376	27.11	27.45
	3	−831.491	51.20	53.60

It is also important to note that experimental data indicates that the KER's that we measure are not single valued. The experimental KER values are the most probable ones from a distribution of values. Since we are using single-point calculations at the optimized geometry of the neutral, the computed values correspond to the most probable value for the KER distribution. The fact that these values are so similar to Coulombic values strongly suggests that electronic structure effects are relatively unimportant for the molecular charge states that are accessed in our experiments.

Figure 5 shows the propensity for the fragmentation of a molecular ion in a given charge state into symmetric and asymmetric product channels. By asymmetric channels we mean those channels in which there are large differences in the charge states of the fragment ions. For example, the (4,1,2) channel is, in this context, considered asymmetric *vis a vis* the (2,3,2) channel. The latter channel would be, in this context, considered as being a symmetric channel.

The energy involved in the fragmentation plays a major role in determining the branching ratio for a given channel. For example, in the case of fragmentation of CS_2^{5+}, the dissociation limit of the symmetric channel (2,1,2) is lower than that of the asymmetric channel (2,2,1), and, consequently, the propensity for fragmentation into the former channel ought to be higher than that for the latter. That this is exactly the case is seen in Fig. 5. It is possible to carry out similar correlations for any charge state using the information provided in Table I and it is confirmed that the branching ratio for symmetric and asymmetric breakup channels appears to be solely governed by energy arguments. An inter-

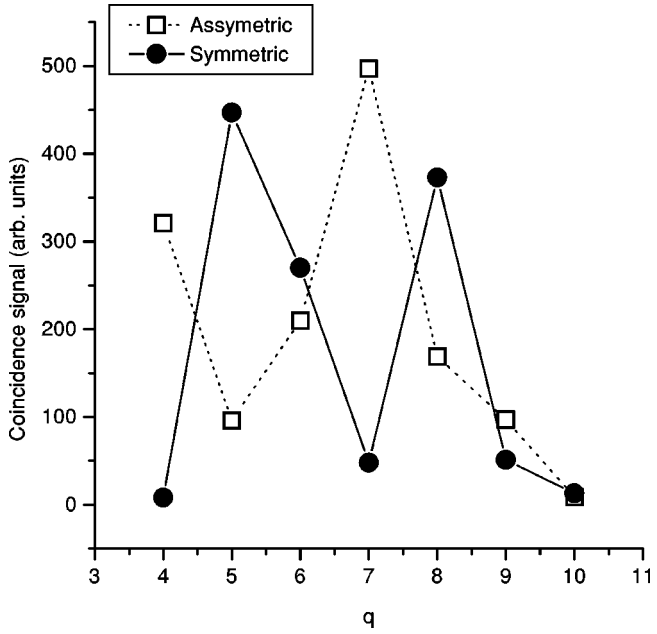

FIG. 5. Propensity for fragmentation into symmetric (solid symbols and solid lines) and asymmetric channels (hollow symbols and broken lines) for different molecular charge states (see text).

esting implication follows. It is known that high-molecular charge states possess a very high density of molecular states. Curve crossing between adiabatic states might be expected to play an important role in the dissociation dynamics such that the minimum energy path is not always the most favored one. The data obtained in our experiments, however, indicates to the contrary that the most exothermic fragmentation pathway is the most favored.

E. Bond angle and χ angle

The angular correlation between the fragment ions may be expressed in terms of the χ angle, which is the angle between the velocity vector of the central *C* ion and the difference between the velocity vectors of the two *S* ions. We also explored the possiblity that it might be possible to gain some insight into whether the dissociation mechanism involving highly charged molecular ions CS_2^{q+} is sequential or simultaneous by probing the distribution of χ angles as a function of ion yield. The χ angle was calculated according to the formula,

$$\chi = \cos^{-1}([u_c(u_{s1}-u_{s2})]/|u_{s1}-u_{s2}|), \tag{2}$$

where u_c, u_{s1}, and u_{s2} are the unit vectors along the dissociating carbon and two sulfur ions, respectively. Physically, the χ angle indicates the direction of the outgoing carbon with respect to the line joining the S-S nuclei.

We further probed the nuclear geometry of the dissociating molecular ion by reconstructing the S-C-S angle (θ_o) from the trajectories of the fragment ions for a single identified dissociation channel. First, the angle θ_v between the velocity vectors of the two outgoing S ions was calculated using the formula

$$\theta_v = \cos^{-1}(u_{s1}u_{s2}) \tag{3}$$

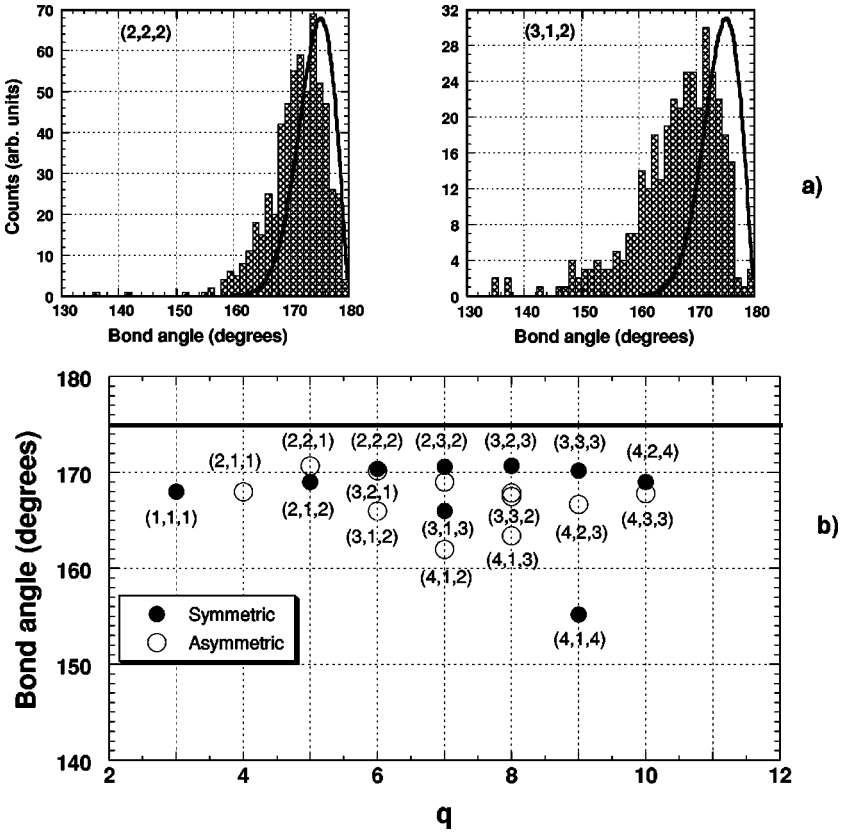

FIG. 6. (a) Histogram depicting reconstructed bond angle distribution for the (2,2,2) and (3,1,2) fragmentation channels, with solid line showing the computed bond angle distribution taking into account zero-point vibration of the degenerate bending mode. (b) Bond angle distribution of the mean values for all the dissociating channels, with solid line indicating the neutral molecule bond angle value of 175.2°.

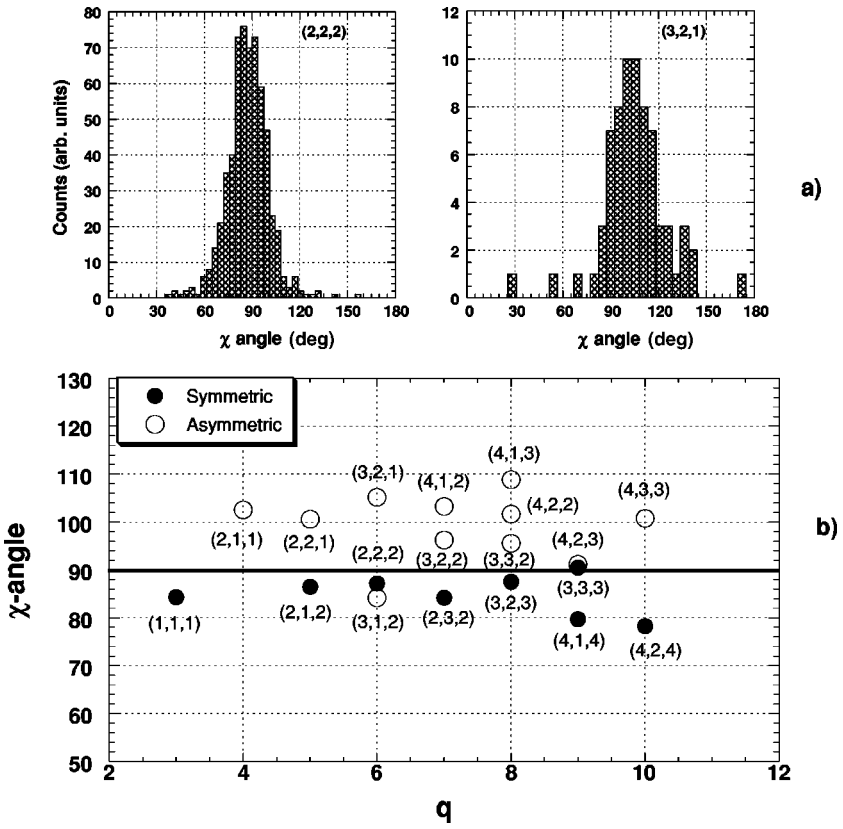

FIG. 7. (b) Histogram depicting the reconstructed χ angle distribution for (2,2,2) and (3,2,1) fragmentation channels. (b) Most probable mean values of the χ angle for all the dissociating channels with solid line at $\chi=90°$ indicating instantaneous fragmentation.

and, then, deducing the bond angle by comparing with simulated data obtained in terms of a plot of angle θ_v against the θ_o.

Figure 6(a) shows histograms depicting the measured bond angle distributions for the (2,2,2) and (3,1,2) fragmentation channels, respectively. Also shown are computed bond angle distributions (solid line) obtained assuming a purely Coulombic fragmentation, with the zero-point vibration of the degenerate bending mode taken into account. The fact that the experimentally determined distributions of bond angles closely follows those predicted from the zero-point vibration of the neutral molecule indicates strongly that the fragmentation occurs instantly in a nonsequential manner.

Figure 6(b) shows mean values of the bond angle distribution for all the dissociating channels. The solid line in Fig. 6(b) indicates the calculated neutral molecule bond angle value of 175.2° and as is seen, the mean distribution of the bond angles are somewhat less and broader than those of the computed neutral distribution. We note that a similar shift was observed in experiments with H_2O [10], but in the opposite direction, towards larger bond angles. In those experiments, the observation that the measured bond angle was larger than that of the neutral, was attributed to be due to the H^+-H^+ repulsion. However, the shift towards smaller bond angles that is observed in the present experiments suggest that the molecular ion is probably excited in the bending mode. We also note that the deviation towards smaller bond angles is more in the product channels where in the charge states of the fragments are largely different and the process energetically unfavorable.

Figure 7(a) shows histograms depicting the measured χ angle distributions for the (2,2,2) and (3,2,1) fragmentation channels. As is seen, the χ-angle values for the symmetric dissociating channels has the most probable value close to 90°. This again confirms our postulate that the fragmentaion is instantaneous, and nonsequential processes appear to be important in the fragmentation dynamics of CS_2^{q+} ions. Figure 7(b) shows the most probable values of the χ angle for all the dissociation channels, as is seen in the figure the χ-angle values for the asymmetric product channels are larger that 90°, which is expected from the fragmentation of a bent molecular systems with different recoil velocities.

V. SUMMARY AND CONCLUSIONS

In this paper we report the results of a study on the fragmentation dynamics of highly charged CS_2 molecules produced in collisions with Ar^{8+} ions at 120 keV energy. These highly charged CS_2^{q+} $(q=3-10)$ ions undergo fragmentation. We measured triple coincidence signals using a TOF spectrometer equipped with a position-sensitive detector that enabled us to measure the velocity components of all the three ionic fragments produced in the fragmentation process. The velocity measurements were used to deduce the total kinetic energy released in the fragmentation of the molecular ion for each particular product channel.

KER values were found to be more or less the same as those predicted by a pure Coulomb explosion, revealing the apparent unimportance of binding electronic interactions in multi-electron systems in high charge states. *Ab initio* quantum computations were carried out to calculate KER values for different fragmentation processes. The calculations were

to the lowest-possible electronic states of a given charge state and represented the lower limit to the expected values. These calculated values were found to be lower than the experimental values, and demonstrate the importance of electronic excitation of the precursor molecular ions in a fragmentation process. The propensity of fragmentation to symmetric and asymmetric channels depends only on the energetics involved in fragmentation channel, with the most exothermic channel being favored.

Velocity vector measurements are also used to obtain the information of the bond angle and χ angle of the molecule prior to fragmentation. The experimentally determined bond angles distribtution closely resembles those predicted from the zero-point vibration of the neutral molecule. The mean values of the reconstructed bond angle is shifted towards smaller values possibly due to the excitation in to the bending mode of the precursor molecular ion. The χ-angle distribution measurement also show that the fragmentation is instantaneous and nonsequential.

ACKNOWLEDGMENTS

The Japanese Society for the Promotion of Science and the Department of Science and Technology, Government of India, are thanked for their support of this collaborative research through the RONPAKU program.

[1] D. Mathur, Phys. Rep. **225**, 193 (1993).

[2] J.E. Biaglow, in *Radiation Chemistry: Principles and Applications*, edited by Farhat Aziz and M.A.J. Rodgers (VCH, New York, 1987), p. 527.

[3] C. Lehman, in *Defects in Crystalline Solids*, edited by S. Amelinckx, R. Grevers, and J. Nihoul (North-Holland, Amsterdam, 1977), Vol. 10.

[4] M. Tarisien, L. Adoui, F. Frémont, D. Lelièvre, L. Guillaume, J.Y. Chesnel, H. Zhang, A. Dubois, D. Mathur, S. Kumar, M. Krishnamurthy, and A. Cassimi, J. Phys. B **33**, L11 (2000).

[5] L. Adoui, C. Caraby, A. Cassimi, D. Lelièvre, J-P. Grandin, and A. Dubois, J. Phys. B **32**, 631 (1999), and references therein.

[6] D. Mathur, E. Krishnakumar, K. Nagesha, V.R. Marathe, V. Krishnamurthi, F.A. Rajgara, and U.T. Raheja, J. Phys. B **26**, L141 (1993); C.P. Safvan and D. Mathur, *ibid.* **27**, 4073 (1994).

[7] D. Mathur, R.G. Kingston, F.M. Harris, and J.H. Beynon, J. Phys. B **19**, L575 (1986).

[8] H. Tawara, T. Tonuma, T. Matsuo, M. Kase, H. Kumagai, and I. Kohno, Nucl. Instrum. Methods Phys. Res. A **262**, 95 (1987), T. Matsuo, T. Tonuma, M. Kase, T. Kambara, H. Kumagai, and H. Tawara, Chem. Phys. **121**, 93 (1988).

[9] J. Ben-Itzhak, S.G. Ginther, V. Krishnamurthi, and K.D. Cames, Phys. Rev. A **51**, 391 (1995), H.O. Folkerts, R. Hoekstra, and R. Morgenstern, Phys. Rev. Lett. **77**, 3339 (1996).

[10] U. Werner, K. Berkford, J. Becker, and H.O. Lutz, Phys. Rev. Lett. **74**, 1962 (1995); Nucl. Instrum. Methods Phys. Res. B **124**, 298 (1997); **98**, 385 (1995).

[11] H. Shiromaru, T. Nishide, T. Kitamura, J.H. Sanderson, Y. Achiba, and N. Kobayashi, Phys. Scr. T **80**, 110 (1999); J.H. Sanderson, T. Nishide, T. Kitamura, H. Shiromaru, Y. Achiba, and N. Kobayashi, Phys. Rev. A **59**, 4817 (1999).

[12] H. Shiromaru, K. Kobayashi, M. Mizutani, M. Yoshino, T. Mizogawa, Y. Achiba, and N. Kobayashi, Phys. Scr. T **73**, 407 (1997).

[13] T. Mizogawa, M. Sato, and Y. Awaya, Nucl. Instrum. Methods Phys. Res. A **366**, 129 (1995).

[14] S. Huzinaga, *Gaussian Basis Sets for Molecular Calculations* (Elsevier, Amsterdam, 1984).

[15] R. Seegar and J.A. Pople, J. Chem. Phys. **65**, 265 (1976).